Positioning Results for LDACS1 Based Navigation with Measurement Data

N. Schneckenburger, B. Elwischger, B. Belabbas, D. Shutin, M-S. Circiu, M. Suess
Deutsches Zentrum für Luft- und Raumfahrt (DLR), Germany

BIOGRAPHIES

Nicolas Schneckenburger received his Dipl.-Ing. (M.Sc) degree in electrical engineering from the University of Ulm, Germany, in 2010. Since then he has been working as a research associate with the Institute of Communications and Navigation at the German Aerospace Center (DLR). His main focus in the last years has been on new communication systems in civil aviation and their utilization for navigation.

Bernard P. B. Elwischger received his Dipl.-Ing. (M.Sc) degree in electrical engineering from Vienna University of Technology, Austria. He was a research assistant at the Institute of Integrated Sensor Systems of the Austrian Academy of Sciences, and wrote his master thesis about the efficiency of positioning algorithms. Currently, he works at DLR in the fields of navigation and synchronization in positioning and timing systems, in particular GNSS.

Boubeker Belabbas is the leader of the integrity group of the Institute of Communications and Navigation at the DLR. He obtained an M.Sc degree in mechanical engineering from the Ecole Nationale Supérieure de lElectricité et de Mecanique in Nancy, France, and a specialized M.Sc in aerospace mechanics from Ecole Nationale Supérieure de lAéronautique et de l'Espace in Toulouse, France.

Dmitriy Shutin received the Ph.D. degree in electrical engineering from Graz University of Technology (TUG), Austria, in 2006. During 2006-2009 he was an assistant professor at the Signal Processing and Speech Communication Laboratory at TUG. From 2009 to 2011 he was a research associate with the Department of Electrical Engineering at Princeton University, USA. Since 2011 he is with the German Aerospace Center. In 2009 he was awarded the Erwin Schroedinger Research Fellowship. He is Senior IEEE Member.

Mihaela-Simona Circiu studied computer engineering at the Technical University Gheorghe Asachi, Romania. She obtained in 2012 a 2nd level specialized M.Sc in navigation and related application from Politecnico di Torino, Italy. Currently, she is a member of the Integrity group of the Institute of Communication and Navigation at DLR. Her main field of work is Ground Based Augmentation System.

Matthias Suess is member of the GNSS systems group of the Institute of Communications and Navigation at DLR. His research focuses on mathematical models of atomic clocks, robust steering and composite clock algorithms using modified Kalman filters. In 2009, he experienced a research visit at the U.S. Naval Observatory to study GNSS timing performances. He graduated as computer scientist with field of specialization in mathematical modelling at the University of Passau, Germany.

ABSTRACT

This paper discusses the validation of the future aeronautical communication system LDACS1 for navigation in order to implement an alternative positioning, navigation, and timing service. The included results originate from flight trials conducted in November 2012.

Within the paper the setup of that measurement campaign is outlined. Results for synchronization of the ground stations, ranging and 2D positioning are presented. Additionally, an estimation of the achievable integrity is given. The obtained results indicate that, if within the measurement area, LDACS1 can be used as APNT system for enroute navigation.

INTRODUCTION

Since the early days of aviation, navigation of the aircraft has always been a crucial and challenging task. Without a reliable estimate of the own position, safe flight operations are not possible. In the last years, navigation solutions which are both highly precise and always available have become even more important in the field of civil aviation: Due to the high level of competition between airline carriers, under the constraint of rising fuel prices, flying the op-

timal, and therefore most efficient route between start and destination equals a large competitive advantage.

Therefore, the entire sector of air traffic management is undergoing a transformation process: In the future, aircraft are to be allowed to fly complete trajectories between start and destination, rather than having a new route assigned, whenever entering a new sector, managed by a different air traffic controller. These principles are usually denoted as "4D trajectories" and have a large potential of decreasing costs for carriers while increasing fuel economy - and therefore having a positive impact on the environment [1].

Despite the immense advantages of those new schemes, they all require better navigational systems than the ones employed previously. In the past decades, navigation for en-route and approach traffic usually relied on two ground-based systems: DME (distance measuring equipment) and VOR (VHF omnidirectional range). Both systems, being more than half a century old, offer only a very limited performance compared to modern GNSS based solutions, e.g. GPS.

Improvements in the field of navigation have been achieved during the last decades using GNSS. These led to certification of flight procedures relying on GPS. To offer an additional degree of integrity, the receivers are usually combined with a ground or satellite based augmentation system (G/S-BAS). Additionally to the current en-route and approach use, employment for CAT-3 landing is planned for the future.

Nevertheless, increased reliance on GNSS brings new challenges with regard to integrity, continuity and availability of the navigation information. The large distances between the aircraft and the transmitting satellites make the system susceptible to interference. Hence, a parallel navigational backup infrastructure, less vulnerable to interference, referred to as alternative positioning, navigation and timing (APNT), needs to be employed. This system can be relied on when GNSS services are temporarily unavailable. As several past incidents show, e.g. the ones in Newark or South Korea, complete unavailability of GPS within a large area may not be a frequent, but still real threat [2, 3].

Currently, different proposals for that backup system are being developed. All employ a ground-based infrastructure to keep the distances between signal transmitters and receiving aircraft minimal. One prominent approach is to intensify use of the DME system. DME uses round trip measurements for range calculation. Nevertheless, this approach suffers from several drawbacks: First of all, a costly extension of the old DME system is required. Secondly, due to the technology available at the time of development, the DME system uses the L-band frequency spectrum very inefficiently. Moreover, the DME pulses are also known to cause interferences to Galileo E5a/E5b and GPS L5 signals [4]. Furthermore, such an extension might severely impact the sustainable use of the L-band for both communications and navigation as foreseen within ICAO. Specifically, the L-band will be used more intensively by DME. This will make it difficult, or even impossible, to allocate sufficient spectrum resources for covering the growing demand for digital communications expected on a mid- and long-term as well as enhance the interference to future GNSS services.

Another prominent approach is to exploit signals of a future system for navigation rather than prolonging dependence on a legacy system. In the last years, the LDACS1 (L-band digital aeronautical communication system - type 1) has turned out to be a likely candidate for the future air-ground communication link. It employs a broadband transmission using orthogonal frequency-division multiplexing (OFDM) and frequency-division duplex (FDD) for forward and reverse channels. Due to the placement of spectral holes between the currently existing DME stations, both systems can well coexist unless the use of DME is not drastically intensified. Specifically, ranges calculated using both systems can be combined to calculate a position, if not enough ranging stations are visible. The main advantage of this proposal is that system infrastructure, that has to be set up in the near future to meet increasing communication capacity requirements, can be employed for both communication and navigation.

To investigate performance possible using LDACS1 for APNT, DLR has set up a project, LDACS-Nav. Firstly, this project includes a theoretical evaluation for using LDACS1 for navigation [5, 6]. A second part of the project is to evaluate the theoretical findings using real measurements. Therefore, in the November of 2012 DLR conducted a flight measurement campaign. The setup consisted of four ground stations and a Falcon 20E aircraft, shown in Fig. 1. Using four stations allows calculation of positions using

Fig. 1: Dassault Falcon 20E (D-CMET) employed in the 2012 measurement campaign.

only the LDACS1 communication signal. First results of the flight trials have been presented in [7].

In the following, we will begin with a brief description of the setup of the LDACS1 measurement campaign. This

includes a basic description of the communication system itself as well at the hardware involved. Next is a detailed description of the algorithms employed. In the following, we show different results: firstly of the synchronization of the ground stations, then on ranges and positions, and finally on integrity. The paper concludes with a summary of the work, a discussion of open issues and an outlook on the future work to be conducted in the field of LDACS1 navigation.

SETUP OF LDACS1 MEASUREMENT CAMPAIGN

In this section a brief overview of the LDACS1 measurement campaign is given. We start with a short introduction of the LDACS1 communication system. Following, the setup of the campaign is outlined. A description of the hardware employed on both aircraft and ground is included.

LDACS1 communication system

LDACS1 is currently one of the most promising candidates for the future air-traffic management (ATM) data link. It is largely based on 4th generation telecommunication technology, and like current system as LTE, it uses OFDM as modulation. It shall be deployed in the aeronautical L-band (960 MHz to 1164 MHz). Compared to the current analog systems, it offers a vastly increased capacity, scalability, and efficiency.

LDACS1 is designed as a cellular system consisting of a network of ground stations (GS). Each GS is assigned a 500 kHz channel. The size of the OFDM discrete Fourier transform (DFT) is 64. Excluding guard bands, 50 subcarriers are available for digital data transmission. Each OFDM symbol, consisting of a useful symbol duration of 102.4 µs (64 samples), is extended with a cyclic prefix (CP) of length 4.8 µs (3 samples). Additionally, a raised cosine windowing function is applied to each OFDM symbol, reducing its out-of-band radiation. This adds another 12.8 µs (8 samples) on each side of an OFDM symbol. Due to the overlapping of the windowing function between consecutive symbols, the overall symbol duration is 120 µs (75 samples). Thus, the overall CP and windowing overhead is about 15 %.

The largest entity in the FL signal is a super-frame (SF) with a duration of $t_{\mathrm{SF}} = 240\,\mathrm{ms}$. Each SF is composed of 2000 OFDM symbols. One SF is made up of several different types of sub-frames, dedicated to the transmission of different information from the GS to the AS. For more information on that topic, the reader is referred to the LDACS1 standard [8]. Table 1 summarizes the LDACS1 parameters.

Measurement campaign setup

The goal of the 2012 flight measurement campaign was to evaluate navigation capability of the future communication system LDACS1. Therefore, to calculate the 3D position of the aircraft as well as the clock offset to the ground, four stations are necessary, unless no other sensors are employed, e.g. barometer. In 2 the positions of the GS in the area south west of Munich are shown. Station A is set up in a measurement van at the airport in Oberpfaffenhofen. Station B is erected on an open area next to a detached house near Marktoberdorf. Station C is installed at a small airport for general aviation pilots in Bad Wörishofen. The last station D is located on a mountain next to a weather station near Peissenberg. The stations are between 30 and 60 km spaced from each other. For its transmission, each GS uses a separate 500 kHz channel in the lower L-band between 965 MHz to 975 MHz, as defined in Table 2 and Fig. 3. Theoretically, no other user is assigned to that band. The closest possible interferes are a TACAN station at the airport in Erding at 962 MHz, and the GSM band below 960 MHz. However, an unidentified interferer was de-

Table 1: LDACS1 transmission parameters

Parameter	Value
Bandwidth	500 kHz
Nominal transmit power	39 dBm
DFT size	64
Subcarriers	50
Subcarrier spacing	≈ 9.7 kHz
Superframe (SF) length	240 ms
OFDM symbols in SF	2000
Sampling time	1.6 µs
Total symbol duration	120 µs
Windowing duration	12.8 µs
Cyclic prefix duration	4.8 µs

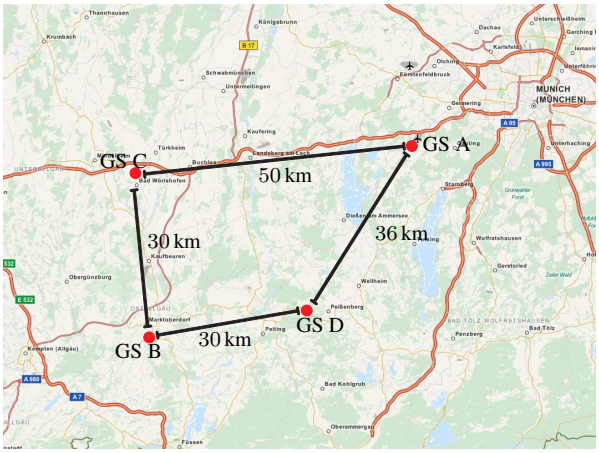

Fig. 2: Ground station locations (©OpenStreetMap).

tected at 970 MHz. Additionally, co-site interference was received from on-board equipment, e.g. DME. The exact positions and frequencies of the stations are provided in Table 2.

Table 2: GS positions and frequencies

Distance [km] from/ to	**A**	**B**	**C**	**D**
A - $f = 973.75$ MHz 48°5'8.91"N, 11°16'37.46"E	-	60	50	36
B - $f = 971.25$ MHz 47°45'5.53"N, 10°38'48.20"E	60	-	30	30
C - $f = 968.75$ MHz 48°0'58.99"N, 10°36'48.63"E	50	30	-	39
D - $f = 966.25$ MHz 47°50'4.57"N, 11°6'59.38"E	36	30	39	-

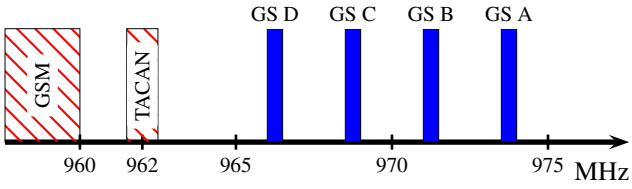

Fig. 3: Frequencies of the stations and adjacent users.

The hardware setup of the ground station is shown in Fig. 4. An Rb atomic clock acts as the common time reference, except for station A where a Cesium clock is employed. A high precision multi frequency GNSS receiver monitors the atomic clocks' offset to the GPS master time. This allows synchronization of the different GS, as described in the following section. The LDACS1 signal is formed by signal generator and amplified using a high power amplifier. Stored in the signal generator is one 240 ms LDACS1 super frame. Every second, the GNSS receiver triggers the transmission of four consecutive frames using a PPS (pulse per second) signal.

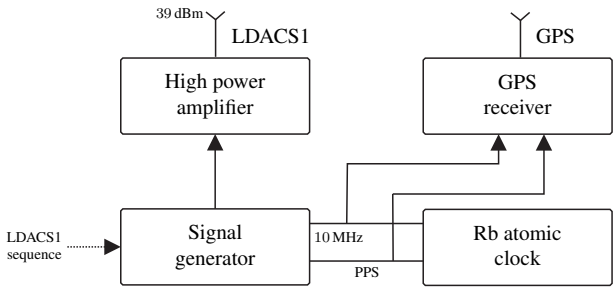

Fig. 4: Schematic ground station hardware setup.

An overview of the hardware setup flown in the Dassault Falcon 20E, shown in Fig. 1, is given in in Fig. 5. Again

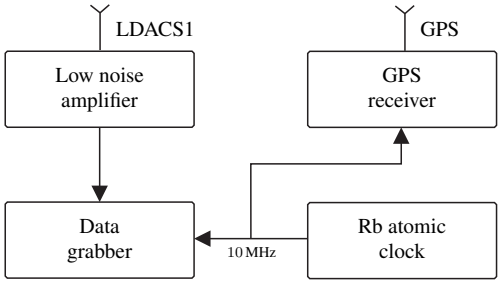

Fig. 5: Airborne station hardware setup.

an Rb atomic clock acts as common time reference. A National Instruments PXIe system is set up as data grabber, simultaneously recording signals, emitted from all ground stations, onto a hard drive. However, to improve signal to noise ratio, directly after the antenna, the received signal is first amplified by a low noise amplifier. The GPS receiver on-board has two tasks: Firstly, as for the ground stations, it compares the Rb time reference to the GPS time. Secondly, and equally important, it acts as a ground truth for the estimated ranges and positions. If an RTK (real time kinematics) solution can be calculated, the accuracy of that ground truth is in the region of centimeters.

The flight trials were conducted in November 2012. Before start and after landing, station A, mounted in a van, met the aircraft on the apron for clock synchronization. The pattern shown in Figure 6 was flown on three different altitudes: FL90 (flight level) ($\approx$ 2900 m), FL310 ($\approx$ 8600 m), and FL390 ($\approx$ 11 560 m). Hereby, the aircraft flew a 'butterfly' pattern over the stations, using each station as turning point. This allows the analysis of different real world geometric constellations. The entire flight took about 90 min.

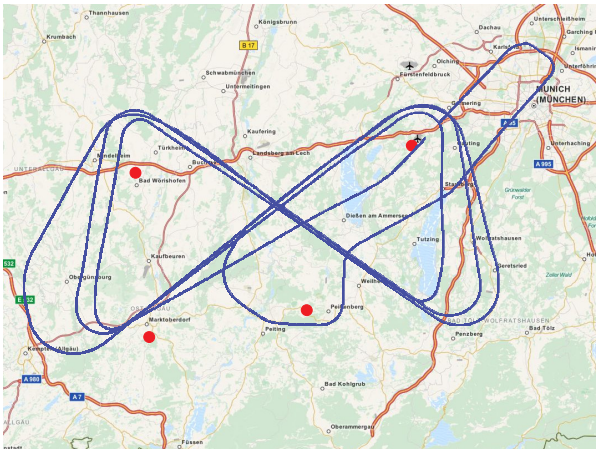

Fig. 6: Route of the flight conducted on 13.11.2012 (©OpenStreetMap).

EMPLOYED ALGORITHMS

In this section we give an overview of the algorithms employed to generate the results in the following section. We start by explaining the ground station synchronization scheme. Following we describe the calculation of the ranges. The section closes with an outline of the employed positioning algorithms as well as the integrity of the positioning results.

Synchronization of ground stations

As outlined in the previous section, the setup of each GS includes one atomic clock. In order to achieve synchronization of the LDACS1 signals emitted by the signal generators of the four GS, a common time base is required. This is accomplished through monitoring of the relative time offsets between those four atomic clocks to GPS system time.

The atomic clock provides a PPS signal and a stable 10 MHz reference signal, which are fed into the signal generator, see Fig. 4. Station A includes a cesium clock, stations B, C, and D are equipped with an oven-controlled Rubidium clocks. In order to maintain clock stability under changing environmental conditions, those three Rubidium clocks are enclosed by an additional chassis providing shock-protection and oven-control. The Rubidium clocks were let run freely during the flight mission, after having been tuned on-site a few days before the start to compensate their deterministic drift values. The steering limits the effect of drift onto the measured time offset relative to GPS system time.

Continuous monitoring of the time offsets between the four atomic clocks is achieved by application of a common-view time transfer method similar to the modified Consultative Committee for Time and Frequency (CCTF) procedure presented in [9]. Through GPS satellite time transfer, the stations' atomic clocks are individually referenced to the atomic clocks of all GPS satellites in view. Dual frequency code measurements in the L1 and L2 bands are used and combined to the ionosphere-free combination P3.

The applied synchronization approach requires calibration of the full time synchronization chain, including all cables, the positions of the four LDACS1 and the four GPS antennas, as well as the four GNSS receivers. The final synchronization accuracy that is achievable by common-view time transfer is dependent on many factors, such as atmospheric or multipath effects. A conservative estimation is given by 10 ns [10].

Calculation of ranges

The evaluation of the data recorded in the aircraft is performed in post processing on the ground. The calculation of the ranges builds the foundation for the estimation of the aircraft's position.

Of fundamental importance for the evaluation of the measurements is the calibration of the entire chain between transmitter and receiver. This is necessary to cancel out error influences caused for example by internal delays or filter characteristics. While the determination of the individual influences would be an elaborate, and in some cases, impossible task, the sum of all influences can be easily calibrated out in one measurement. Therefore, the final and complete setup is arranged. In a transmitter-receiver calibration measurement, the antenna connector of the transmitter is directly connected to the antenna input of the receiver. This measurement provides a zero distance calibration: Neglecting antennas delays, the receiver records the equivalent of a $0\,\mathrm{s}$ delay signal. That means we are able to calibrate out all systematic errors caused by the receiver and transmitter hardware (excluding antennas).

For the calculation of the pseudoranges to all stations, we use a standard correlator: Hereby, we correlate the received signal with the recorded calibration signal on an OFDM symbol basis. The calculation is performed in the time domain, since this has proven less vulnerable towards wide band interference by other equipment on-board the aircraft, e.g. DME.

To calculate true ranges from pseudoranges, the offset between two involved clocks has to be present, i.e. the exact offset between the clock on ground and in air has to be known[1]. Therefore, the offset between the two atomic clocks is measured both at the start and landing. Unfortunately, the drift of an atomic clock under the influence of vibrations or temperature and pressure changes, like the one experienced in the aircraft during flight, may not be necessarily linear. Therefore, to ensure detectability of a nonlinear drift, the offset between the frequency standard and GPS time is continuously monitored during the flight by a GPS receiver. Fortunately, as shown in Fig. 7, the clock drift has indeed turned out to be almost linear. During the $100\,\mathrm{min}$ of flight time, the clocks drifted about $400\,\mathrm{ns}$ in respect to each other. If the offset between the two clocks is subtracted from the pseudoranges, they become true ranges. For that subtraction a filtered version of the raw offsets is used, as shown in Fig. 7.

For more information on the calibration and synchronization of the aircraft and ground clock, the reader is referred to [11].

Calculation of positions

Having the pseudoranges observed from each station, we use a multilateration algorithm to estimate the position of the user. Two possible approaches are investigated:

- The iterative approach based on the Newton-Raphson algorithm. This runs perfectly as long as the initial

[1]Note however, that this is only necessary, if individual ranges are to be evaluated. For calculation of positions this step is not mandatory, since, as described in the following section, the algorithm only requires pseudoranges.

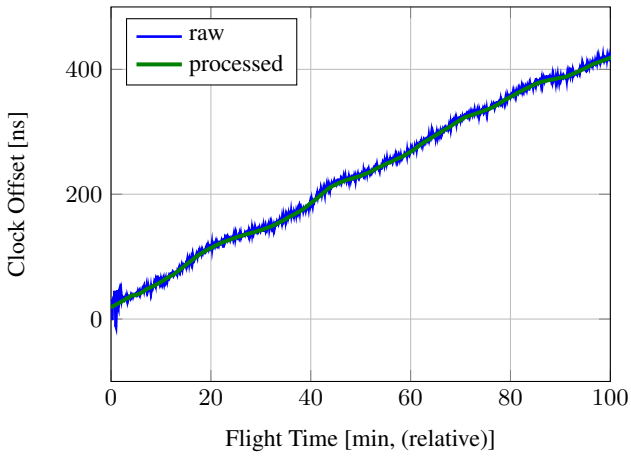

Fig. 7: Drifting of the aircraft clock in respect to the clock at GS A during flight.

guess (the last GNSS position fix for example) is close to the true position, and the pseudoranges error variance is not too large.

- A direct method consisting of solving the position without iterating. This will be the preferred method for a real time implementation.

In our case, the "true" position was known with a high confidence by using post processing dual frequency GPS measurements.

For a proof of concept, it is sufficient to investigate the deviation of the pseudoranges to the truth and to see the impact in the position of errors in the pseudoranges. We assume that the service targeted is non precision approach and corresponds to Required Navigation Performance of 0.3 NM (RNP 0.3) where a vertical guidance can be done using a barometric altimeter with an error of 10 meters (one standard deviation). This enables us to determine a position with 3 stations if the user clock bias is considered as an unknown. During the flight trial, 4 stations were available which lets one degree of freedom for a consistency check as in RAIM (Receiver Autonomous Integrity Monitoring). Though the 3D problem is reduced to a horizontal positioning service. It is therefore sufficient to estimate the east and north component of the position with respect to a reference point. We define the pseudorange observation vector as $\rho(t) = (\rho_A(t)\,\rho_B(t)\,\rho_C(t)\,\rho_D(t))^T$, and $x_{ENt} = (x_{east}(t)\,x_{north}(t)\,b(t))^T$, where b represents the user clock bias with respect to a system time. We have the following relation:

$$\rho(t) = G x_{ENt}(t) + \epsilon \tag{1}$$

Where G is the geometry matrix representing the line of sight unit vector in east and north coordinates for each station and a column of ones corresponding to the user clock bias (each pseudorange contributing with the same weight to the determination of the clock bias). ϵ is the vector of pseudorange errors including time synchronization error, propagation errors (troposphere, multipath) and the receiver noise error while estimating the pseudoranges. The error considered is overbounded by a Gaussian distributed random vector. As a linear over determined system, the solution (best estimate) of the linearized multilateration problem can be expressed as follows:

$$x_{ENt} = \left(G^T W G\right)^{-1} G^T W \rho \tag{2}$$

With W being a weighting matrix corresponding for example to the inverse of the covariance of the pseudorange errors. The solution is the one which minimizes the least squares error in the case of Gaussian distributed errors. Otherwise it is just an approximation.

RESULTS

In this section the results from the measurement campaign are presented. Due to its importance for all following results, we first take a look on the synchronization of the ground stations. This is followed by the results for the ranging, which are then used for calculation of the positions. The section concludes with results on the integrity of navigation using LDACS1.

Clock synchronization

The monitoring of the station clocks during the flight mission worked successfully, without gaps or outliers. This is illustrated by Fig. 8, which shows the relative time offsets of the stations. The time offsets are shifted to zero at the start time of the flight measurement, to allow their linear growth to be compared. The linear fit indicated by dashed

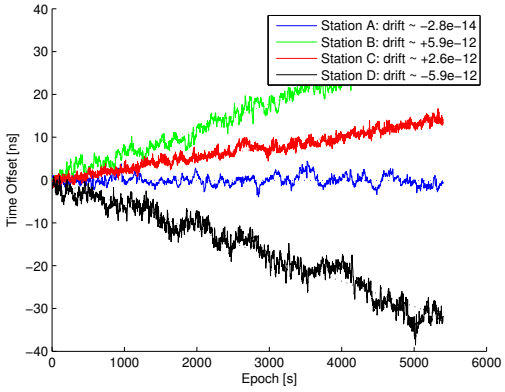

Fig. 8: Station clocks relative to GPS time, normalized to zero.

lines gives an estimate of the drift of the clocks, i.e., their linear growth with respect to GPS time. The drift is in the range of $\pm 5.9 \cdot 10^{-12}[s/s]$ for the Rubidium clocks, and

at the level of $10^{-14}[s/s]$ for the Cesium clock. These are typical values for such clock types and furthermore a result of the steering.
The corresponding overlapping Allan deviation is illustrated in Fig. 9. To separate the contribution of observation noise and the clocks to the Allan deviation, we compare it to the lower bound of the Rubidium clocks' white frequency noise (sloping down with -1/2) as well as to a conservative upper bound of white observation noise (sloping down with -1 [12]). Thus, the observed Allan deviation is dominated by measurement noise originating from the applied time transfer technique. Through extrapolation the white noise is estimated to be about 1 to 2 ns.

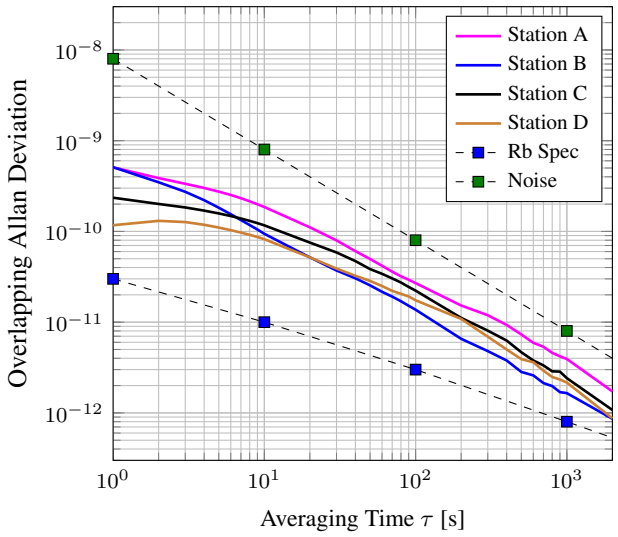

Fig. 9: Observed Allan deviation of the station clocks.

Ranging

The calculation of the pseudoranges is a prerequisite for positioning and is therefore of high importance. For better illustration, the clock offset, still present in pseudoranges, was removed, as described in the previous section. Thus, we are dealing with true ranges now, rather than only pseudoranges. For the analysis of the ranging performance, we look at three 120 s segments, taken at different flight levels: FL100 (2900 m), FL280 (8600 m), and FL380 (11 560 m). The segment used lies in the center of the measurement area, as shown in Fig. 10. In Fig. 11 the distribution for the errors for each altitude as well as mean error and RMSE are shown. The RMSE is defined as

$$\mathrm{RMSE} = \sqrt{\frac{1}{N}\sum_{i=1}^{N} \mid \hat{\rho}_{i,\mathrm{est}} - \hat{\rho}_{i,\mathrm{ref}} \mid^2} \qquad (3)$$

with $\hat{\rho}_{i,\mathrm{est}}$ and $\hat{\rho}_{i,\mathrm{est}}$ being the i^{th} true range by the estimator and the GPS reference, respectively. In Fig. 11, a

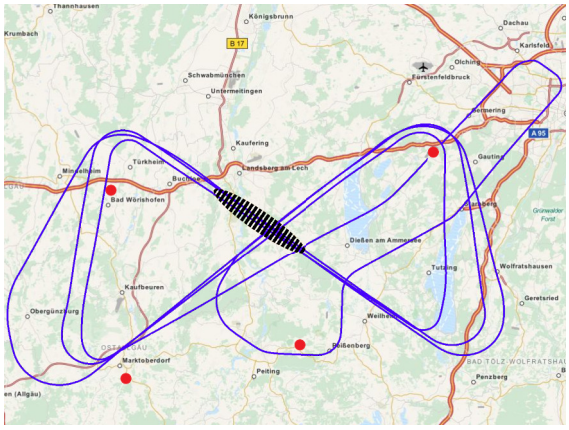

Fig. 10: Segment for range calculation results.

large dependence of the error on the altitude can be observed. While for the two higher altitudes, FL280 and FL380, the RMSE is around 10 m, for the lowest flight level it is well above 40 m. A difference can also be observed in the shapes of the error distributions. The distribution for FL380 is a clean Gaussian around the mean $\mu = 6.7$ m. Similarly, for FL280 the distribution looks almost Gaussian, however it is slightly more off center of the mean error of $\mu = 7.2$ m. The distribution for the lowest flight level exhibits no resemblance with a Gaussian, it rather looks like a mixture of several Gaussian distributions. Additionally, a bias of up to 11.8 m can be observed. This effect is mainly attributed to tropospheric effects.

As this was a measurement campaign with a real world measurement data, it is hard to determine the reason why for such strong performance degradation at lower altitudes. However, we strongly suspect this behavior to be caused by multiple propagation paths between the ground and airborne station. Two main reasons exist for this hypothesis: Firstly, in contrast to GNSS, the receiving antenna is pointing downwards. Hence, all propagation paths originating from the ground are received by the antenna. Secondly, several scatterers exist around the stations.

To prove assumption of multiple propagation paths, a novel sparse super resolution algorithm (VB-SPE, variational Bayesian sparse parameter estimation) [13] is combined with a Kalman filter. By this means, the VB-SPE first extracts the different multipath components from the signal. The Kalman filter then tracks all multipaths over time and decides on the direct line of sight path. The entire algorithm is denoted as sparse adaptive multipath estimation (SAME).

Fig. 12 shows the estimated range for a short segment at FL280.

The standard correlator yields to errors exceeding 50 m. Running the SAME algorithm however shows, that the signal is received from several multiple propagation paths. Since they most likely originate from buildings around the transmit antenna, they have only a delay of a few hundred

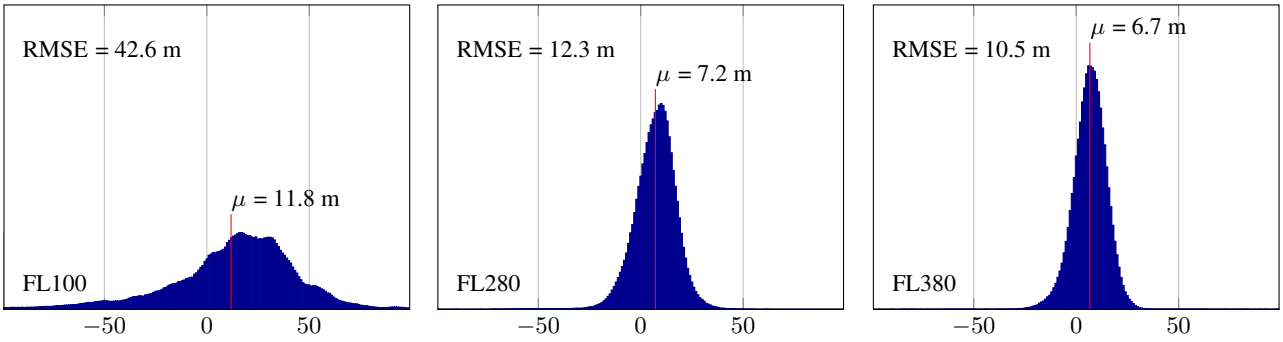

(a) Estimation error [m] (b) Estimation error [m] (c) Estimation error [m]

Fig. 11: Range error distribution, mean error, and RMSE for (a) FL100, (b) FL280, and (c) FL380.

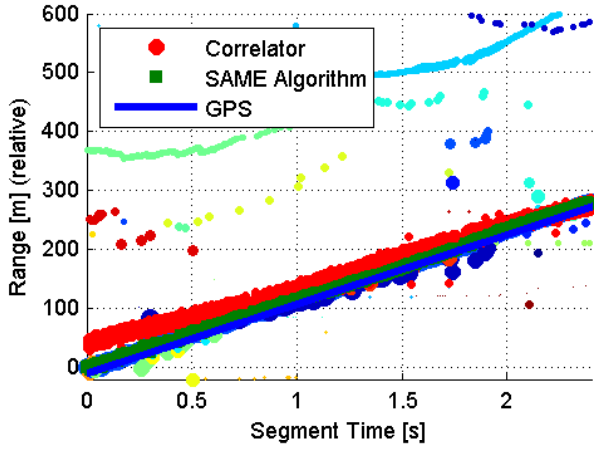

Fig. 12: Application of SAME algorithm to find multiple propagation paths and tracking of line of sight path.

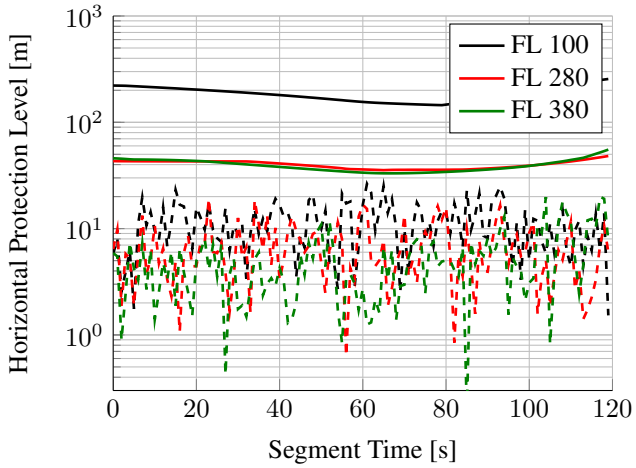

Fig. 13: HE and HPL with 10^{-5} Integrity risk at different flight levels.

meters compared to the line of sight. Keeping in mind, that at a sampling rate of 625 ksamples per second, the duration of one sample equals 480 m. This means the multipaths can be spaced less than one sample from the direct path, which makes their resolution a very challenging task. Nevertheless, the algorithm can cope with that situation. With the different propagation paths being detected, the error is significantly reduced from an RMSE of 30.5 m with a standard correlator to 7 m with the SAME algorithm.

Positions

For the period of interest, we have estimated the horizontal error based on the classical multilateration algorithm. Additionally we have plotted the HPL corresponding to the 10^{-5} quantile. Figure 13 shows the horizontal positioning errors and the protection levels at different flight levels.

Integrity

The integrity concept adopted here is based on a Gaussian overbound of the pseudorange error calculated using a quantile quantile plot method. The overbound is done for every class of elevation angle considering constant number of samples per elevation class. The resulting curves are used to estimate the horizontal protection levels (HPL), a position bound corresponding to an integrity risk quantile. Usually for RNP an integrity risk of 10^{-5} per hour is considered. In Figure 14 the standard deviation of the range errors and the corresponding overbounds are plotted. Different colors correspond to different flight levels. The large errors at low altitudes induce large sigma overbounds (black curves) impacting the protection levels. The best results are obtained when the aircraft was flying at an altitude of 8600 m (FL 280, red curve).

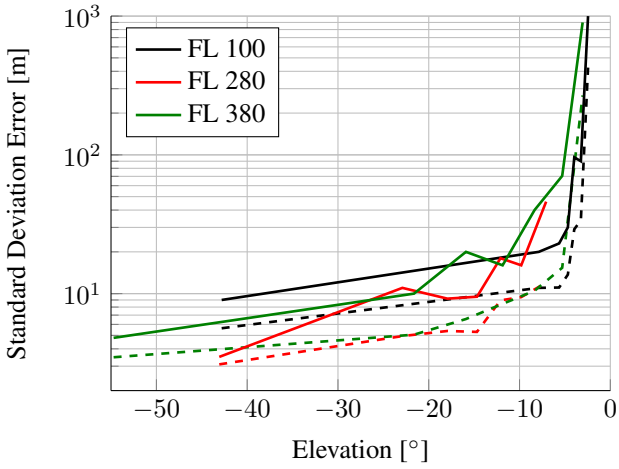

Fig. 14: Range error overbounds at different flight levels.

CONCLUSIONS

In this paper, we gave an assessment of the navigation performance using the future aeronautical communication system LDACS1. The results presented in this paper are generated using data obtained during a measurement campaign in 2012. One of the major challenges during the campaign is the synchronization of the ground stations. Using GPS common view time transfer, the ground stations are synchronized to nanosecond precision. The synchronization is achieved without gaps or outliers, and clock drifts and stability are as expected.

Results for unprocessed ranges indicate a significantly higher RMSE for lower altitudes compared to the higher flight levels. This effect is attributed to the existence of strong multiple propagation paths. Using a sophisticated multipath detection algorithm the different propagation paths may be separated and the RMSE significantly reduced. The overall range RMSE of the entire measurement is 16 m.

The position algorithm needs to be adapted due to the nonlinearity of the multilateration concept (short ranges and large errors). In that case a direct method will be selected and implemented to work for real time APNT. The integrity concept suggested here is based on a Gaussian overbound of the observed errors. It appears that for low elevation angles, the magnitude of errors can reach hundreds of meters which inflate in a large amount the protection levels. Methods to reduce the pseudorange errors are under investigation - especially multipath mitigation techniques and consideration of a mask angle for the stations experiencing strong multipath at low elevation. The last solution limits strongly the availability of the ranging source especially for aircraft flying at low altitude. An additional aspect not taken into account in this study is the development of monitors either imbedded in the ground stations or on board the aircraft to detect and flag faulty ranging sources. A better knowledge of the ranging threats based on additional flight trials will be necessary. The integrity concept although very simple provides very promising results and will improve based on the better knowledge of the system and the characteristics of the ranging errors.

Nevertheless, several challenges are still to be addressed in future research. Firstly, a strong bias can still be found in the ranges. This is mainly attributed to the influence of tropospheric effects, which may be corrected using an advanced model for the troposphere. The algorithm for the detection of multipath has to be improved in order to work on the entire set of data. Alternative synchronization methods for the ground stations are still under investigation [14, 15]. Finally, the integrity concept has to be improved in order to show, under which geometries and altitudes LDACS1 can act as an APNT system for en-route navigation.

ACKNOWLEDGMENTS

The authors would like to thank the entire Institute of Communication and Navigation and the Institute of Flight Experiments for their continuous help, support and guidance. The authors are especially grateful for the great work of Michael Walter, Christian Hauswurz, Werner Rox, Martin Hammer, Hong Quy Le, Hazem Elsayed, Michael Schnell, Johann Furthner, Uwe-Carsten Fiebig, Michael Meurer, and Christoph Günther. Special thanks go to the staff at the 'Observatorium Hohenpeissenberg' of the German weather service (DWD), especially to Fritz Schönenborn, Claudia Unterreiner in Marktoberdorf, and Günter Schmid from 'Flugplatz Bad Wörishofen'. Without their support the setup of the ground stations would have not been possible. Thanks also go to TimeTech GmbH, Stuttgart, for their rapid provision of measurement equipment and Rücker Aerospace GmbH, Oberpfaffenhofen, for their support during the aircraft certification process.

REFERENCES

[1] Roger-wilco.net, "4D Trajectory Management What is this?," 2012.

[2] GPSWorld.com, "Massive GPS Jamming Attack by North Korea," 2012.

[3] B. J. C. Grabowski, "Personal Privacy Jammers : Locating Jersey PPDs Jamming GBAS Safety-of-Life Signals," 2012.

[4] G. X. Gao, "DME/TACAN Interference and its Mitigation in L5/E5 Bands," in *20th International Technical Meeting of the Satellite Division of The Institute of Navigation (ION GNSS)*, (Fort Worth, TX, USA), 2007.

[5] N. Schneckenburger, D. Shutin, and M. Schnell, "Precise aeronautical ground based navigation using

LDACS1," in *Integrated Communications Navigation and Surveillance Conference Proceedings (ICNS)*, (Washington DC, USA), 2012.

[6] B. Belabbas, M. Felux, M. Meurer, N. Schneckenburger, and M. Schnell, "LDACS1 for an Alternate Positioning Navigation and Time Service," in *GNSS Signals*, (Toulouse, France), 2011.

[7] N. Schneckenburger, B. P. B. Elwischger, B. Belabbas, D. Shutin, M.-s. Circiu, M. Suess, M. Schnell, J. Furthner, and M. Meurer, "LDACS1 Navigation Performance Assessment By Flight Trials," in *The European Navigation Conference*, (Vienna, Austria), 2013.

[8] M. Sajatovic, B. Haindl, C. Rihacek, M. Schnell, U. Epple, and S. Brandes, "L-DACS1 System Definition Proposal: Deliverable D3 - Design Specifications for L-DACS1 Prototype." 2009.

[9] P. Defraigne, C. Bruyninx, and N. Observatory, "Time Transfer to TAI using Geodetic Receivers," *Metrologia*, vol. 40, pp. 184–188.

[10] D. W. Allan and M. A. Weiss, "Wj 07703,," in *34th Annual Frequency Control Symposium*, no. May, (Ft. Monmouth, NJ, USA), pp. 334–346, 1980.

[11] D. Shutin, N. Schneckenburger, M. Walter, and M. Schnell, "LDACS1 Ranging Performance - An Analysis of Flight Measurement Results," in *IEEEAIAA 32th Digital Avionics Systems Conference (DASC)*, (Syracuse, NY, USA), 2013.

[12] D. W. Allan, "Time and Frequency (Time-Domain) Characterization, Estimation, and Prediction of Precision Clocks and Oscillators," *IEEE Transactions on Ultrasonics, Ferroelectrics and Frequency Control*, vol. 34, no. 6, pp. 647–654, 1987.

[13] D. Shutin, W. Wang, and T. Jost, "Incremental Sparse Bayesian Learning for Parameter Estimation of Superimposed Signals," in *10th International Conference on Sampling Theory and Applications*, no. 1, (Bremen, Germany), pp. 6–9, 2013.

[14] M. Suess, B. Belabbas, J. Furthner, and M. Meurer, "Robust Time Synchronization Methods for Future APNT," in *ION GNSS+*, (Nashville, TN, USA), 2012.

[15] M. Suess, B. Belabbas, and M. Meurer, "Joint Positioning and Time Synchronization for Future APNT," in *ION GNSS+*, (Nashville, TN, USA), 2013.